

Estimation of a Cover-Type Change Matrix From Error-Prone Data

Steen Magnussen¹

Abstract.—Coregistration and classification errors seriously compromise per-pixel estimates of land cover change. A more robust estimation of change is proposed in which adjacent pixels are grouped into 3×3 clusters and treated as a unit of observation. A complete change matrix is recovered in a two-step process. The diagonal elements of a change matrix are recovered from estimates of the temporal correlations of cover-type frequencies and an estimate of the odds-ratio of no change. Off-diagonal elements are recovered from least-squares solutions to a set of constrained linear equations. The proposed method produced less biased estimates on three of five sites when the average coregistration error was in excess of 0.3 to 0.7 pixels and on four of five sites if classification accuracy is below 0.9.

Introduction

Land cover change estimation from remotely sensed data is riddled with a unique set of problems due to registration errors when two images are coregistered (Coppin and Bauer 1996, Coppin *et al.* 2004) and classification errors (Congalton 2001, Pontius Jr. and Lippitt 2006). A registered change in a unit can therefore misrepresent the actual change event. Although techniques for reducing the bias due to classification errors are readily available (Czaplewski 2003, Stehman and Czaplewski 1998), their efficiency depends critically on an accurate estimate of a confusion matrix for all change classes; a reality that is rarely met.

This study proposes a new method for estimating a $K \times K$ change matrix \mathbf{C} for K cover types from clusters of pooled

pixels instead of individual pixels. Change estimated from clusters of spatially adjoining units is assumed to be less sensitive to the problems stated previously than a per-pixel estimation. Clusters must be large enough to mitigate the effect of the aforementioned problems, yet small enough to reduce the loss of information that occurs when pixels are pooled. A cluster of 3×3 pixels is chosen as a compromise.

Estimates of no change on the main diagonal of a change matrix $\mathbf{C}_{kk}, k = 1, \dots, K$ are recovered from temporal correlation coefficients of cluster-level pixel counts and the odds ratio of no change (Magnussen 2004). Off-diagonal elements are recovered by least-squares solutions (CLS) to a set of linear constraints.

The performance of the proposed method is assessed for a 4×4 change matrix with data from five sites. Coregistration and classification errors are simulated across of a range of specifications. For a detailed version of this study, see Magnussen (2007).

Material and Methods

Recovery of the change matrix begins with a complete tessellation of the coregistered and the classified time 1 (t_1) and time 2 (t_2) images into M size 9 clusters with pixels in a 3×3 array. Only cluster-level counts of the number of pixels in each class at t_1 and t_2 will be used for the recovery. Specifically, the t_1 data are $\mathbf{n}_1^{(i)} = [n_{1+}^{(i)}, \dots, n_{K+}^{(i)}, i]_{i=1, \dots, M}$, where $n_{k+}^{(i)} = \sum_{k'} n_{kk'}^{(i)}$; i.e., the k th row sum of \mathbf{n}_i is the number of class k units in the i th cluster at time t_1 ; likewise, t_2 data are $\mathbf{n}_2^{(i)} = [n_{1+}^{(i)}, \dots, n_{K+}^{(i)}, i]_{i=1, \dots, M}$, where $n_{k+}^{(i)} = \sum_{k'} n_{kk'}^{(i)}$. The state of the population at t_1 and t_2 is captured by the vectors $\mathbf{n}_1 = [n_{1+}, n_{2+}, \dots, n_{K+}]$ and $\mathbf{n}_2 = [n_{1+}, n_{2+}, \dots, n_{K+}]$. The total number of pixels is $\sum_k n_{k+} = \sum_k n_{+k} = n_{++}$.

¹ Research Scientist, Natural Resources Canada, Canadian Forest Service, 506 West Burnside Road, Victoria BC, V8Z 1M5, Canada. E-mail: steen.magnussen@nrcan.gc.ca.

Recovery of the Main Diagonal of the Change Matrix

A procedure for the recovery of the main diagonal in the change matrix has been detailed by Magnussen (2004). First, Pearson's correlation coefficients ρ_{kk} of $n_{kk}^{(i)}$, $i = 1, \dots, M$, $k = 1, \dots, K$ are computed. From these coefficients, an estimate \tilde{n}_{kk} is obtained, as outlined by Murtaugh and Phillips (1998). A second estimate $\tilde{\tilde{n}}_{kk}$ is obtained by finding an odds ratio of no change for class k ($\equiv n_{kk} \sum_{k \neq k'} n_{k'k'} \times \frac{n_{kk} - n_{k'k'}}{n_{kk} - n_{k'k'}}$) (Fleiss 1981) that maximizes the likelihood of the observed counts $n_i^{(i)}$, $i = 1, \dots, M$, $t = 1, 2$ (Magnussen 2004). A linear combination of these two estimates is used as the final estimate—specifically, $\hat{n}_{kk} = \frac{2}{3} \tilde{n}_{kk} + \frac{1}{3} \tilde{\tilde{n}}_{kk}$.

Recovery of Off-Diagonal Elements in the Change Matrix

Recovered off-diagonal elements $n_{kk'|k \neq k'}$ are CLS to a set of constrained equations. From n_{++} and the previous estimates of \hat{n}_{kk} , we can formulate a trivial set of $K \times K$ constraints on the row and column sums of the elements in the change matrix. If we were to recover the off-diagonal elements in a 3×3 change matrix, we could formulate a rank five set of constraints for the six off-diagonal elements. The ratio of unknowns (6) to the rank of the linear constraints (5) is the maximum possible. Hence, if we could reduce the recovery problem to a 3×3 change matrix, the CLS recovery would be the best possible. For a $K \times K$ change matrix, we can create $Bin(K, 3)$ 3×3 change matrices and find a set of 14 linear constraints on their off-diagonal elements with a maximum possible rank of 9 and then find the CLS solution by least squares (Magnussen 2007). All CLS estimates satisfy: $\hat{n}_{kk'}^{CLS} \geq 0$, $\sum_{k,k'} \hat{n}_{kk'}^{CLS} = n_{++}$, and $n_{kk'} \supset \text{Integer}$, $k, k' = \{1, \dots, K = 4\}$.

Performance Assessment

In five case studies with four land-cover classes ($K = 4$), the recovered change matrix $\hat{\mathbf{n}}_{CLS}$ is compared to the actual matrix $\hat{\mathbf{n}}$ obtained by a direct counting (DIR) of pixel-level change. To facilitate a Monte Carlo simulation of errors of coregistration and classification (see the next section), the assessment is carried out with data from 200 replications of simple random sampling of $m = 200$ 3×3 clusters with and without errors.

Monte Carlo Simulation of Coregistration and Classification Errors

Eleven levels of average coregistration errors in t_2 data were simulated at the cluster level. With a probability of P_0 , the “true” data in a 3×3 cluster had no coregistration error ($\in [0, 0.1, \dots, 0.9, 1.0]$). With a probability of $P_1 = \frac{2}{3} P_0$, the location of a cluster was either shifted one column to the left (right) or one row up (down). With a probability of $P_2 = \frac{1}{3} P_0$, the location of a cluster was shifted one column to the left (right) or one row up (down). Registration errors in each of the 200 replications of a random sample of 200 clusters were distributed at random across clusters.

Classification errors at t_1 and t_2 were assumed to be equal and independent. The following symmetric 4×4 confusion matrix \mathbf{P} was used to simulate multinomial classification errors:

$$\mathbf{P} = \begin{bmatrix} & \text{True} = 1 & \text{True} = 2 & \text{True} = 3 & \text{True} = 4 \\ \text{Clsf.} = 1 & p_{k|k} & \frac{17}{24}(1 - p_{k|k}) & \frac{5}{24}(1 - p_{k|k}) & \frac{2}{24}(1 - p_{k|k}) \\ \text{Clsf.} = 2 & \frac{17}{24}(1 - p_{k|k}) & p_{k|k} & \frac{5}{24}(1 - p_{k|k}) & \frac{5}{24}(1 - p_{k|k}) \\ \text{Clsf.} = 3 & \frac{5}{24}(1 - p_{k|k}) & \frac{2}{24}(1 - p_{k|k}) & p_{k|k} & \frac{17}{24}(1 - p_{k|k}) \\ \text{Clsf.} = 4 & \frac{2}{24}(1 - p_{k|k}) & \frac{5}{24}(1 - p_{k|k}) & \frac{17}{24}(1 - p_{k|k}) & p_{k|k} \end{bmatrix} \quad (1)$$

The value of $p_{k|k}$, the classification accuracy, was varied from 0.5, 0.6, ..., 0.9 with the value fixed during one simulation.

Examples

Remotely sensed data from five large forested areas (BC, HI, IT, NB, SE), representing different regional landscapes with contrasting cover-type composition and rates of presumed change, are used for demonstrating the performance of the proposed alternative estimator of a change matrix when data are potentially error-prone. The data domains vary in size from 109 km² (BC) to 188 km² (IT). Details are in Magnussen (2004). Population sizes in pixels of approximately 30×30 m were 121,104 (BC), 129,600 (HI), 208,675 (IT), 181,068 (NB), and 166,464 (SE). An example of a population change matrix for IT is in table 1.

Table 1.—True change matrix for IT.

Class	1	2	3	4	All (t_i)
1	30771 (14.7)	89 (0.0)	5117 (2.5)	4262 (2.0)	40239 (19.3)
2	2 (0.0)	1455 (0.7)	80 (0.0)	12 (0.0)	1549 (0.7)
3	3582 (1.7)	3321 (1.6)	64977 (31.1)	1876 (0.9)	73756 (35.3)
4	630 (0.3)	30 (0.0)	364 (0.2)	92107 (44.1)	93131 (44.6)
All(t_2)	34985 (16.8)	4895 (2.4)	70538 (33.8)	98257 (47.1)	208675 (100.0)

Notes: Table entries are number of pixels. Numbers in parentheses are percentages of the total. Percentages may not add to 100 due to rounding.

Results

Only results pertaining to IT are given. Diagonal elements of $\hat{\mathbf{n}}_{CLS}$ estimates were generally estimated with less bias than off-diagonal elements; a trend that is especially clear on a relative scale where the bias of diagonal estimates was one-half to one-tenth of the bias in off-diagonal change estimates. Relative bias of estimated diagonal elements was in the range of 5 to 10 percent. Scatter-plots in figure 1 give additional insight to CLS performance. For the diagonal elements, the relationship to DIR was typically linear with $0.97 \geq \hat{R}_{adj}^2 \geq 0.91$, yet with a persistent bias. For the off-diagonal elements, the scatter plots suggest a linear relationship but also a persistent bias.

Coregistration errors in t_2 data introduce bias in $\hat{\mathbf{n}}$ and increased the bias in $\hat{\mathbf{n}}_{CLS}$. As the coregistration error increases, however, the bias increased three to four times faster in $\hat{\mathbf{n}}$ than in $\hat{\mathbf{n}}_{CLS}$ (fig. 2). As a result, when the average coregistration error reaches 0.3, one can expect less bias in the diagonal elements in $\hat{\mathbf{n}}_{CLS}$ than in $\hat{\mathbf{n}}$. A similar situation arises for the off-diagonal elements when the average coregistration error exceeds 0.4.

Classification errors also generate a serious bias in $\hat{\mathbf{n}}$ and $\hat{\mathbf{n}}_{CLS}$ (fig. 3). As expected, diagonal elements are most sensitive to classification errors because a classification error generates a change event where none occurred. The rate at which bias increased as classification accuracy decreased was about 1.5 times higher in $\hat{\mathbf{n}}$ than in $\hat{\mathbf{n}}_{CLS}$. The critical accuracy level below which $\hat{\mathbf{n}}_{CLS}$ would be less biased than $\hat{\mathbf{n}}$ is around 0.9.

Figure 1.—Scatter plot of $\hat{\mathbf{n}}_{kk'}^{CLS}$ versus $\hat{\mathbf{n}}_{kk'}$ in 200 replicated samples of size 200 in IT.

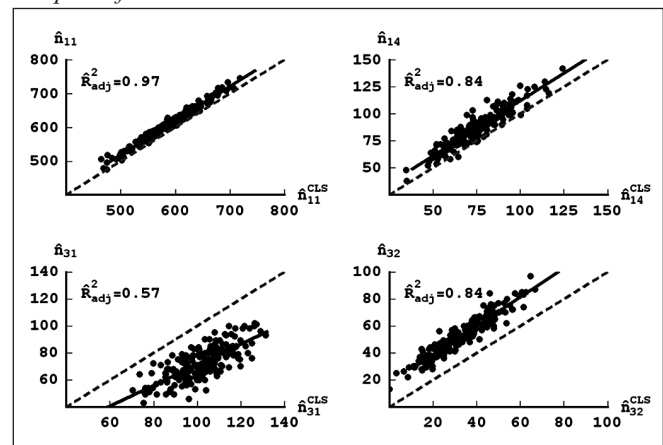


Figure 2.—Mean absolute bias (MAD) of elements of $\hat{\mathbf{n}}_{CLS}$ and direct counts $\hat{\mathbf{n}}$ (DIR) plotted against average coregistration error (unit: pixel of 30×30 m).

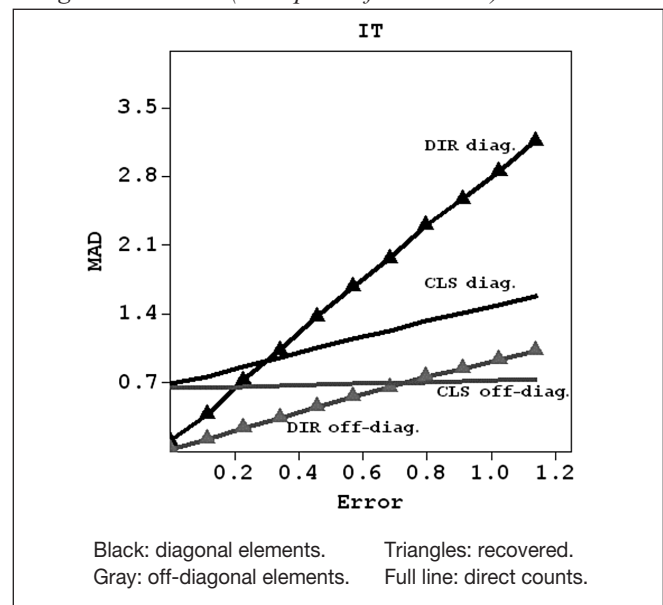
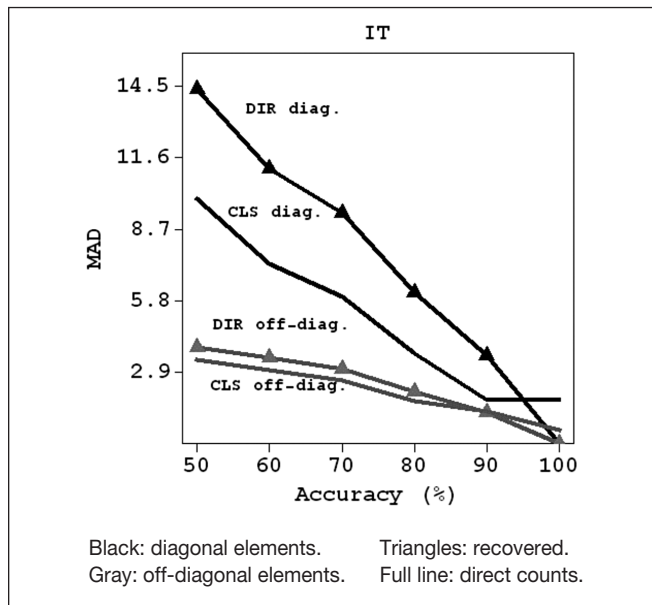


Figure 3.—Mean absolute bias (MAD) of elements of $\hat{\mathbf{n}}_{CLS}$ and direct counts $\hat{\mathbf{n}}$ (DIR) plotted against classification accuracy.



Discussion

A change matrix recovered from cluster-level counts of units per class at two points in time is, in absence of registration and classification errors, less accurate than a change matrix obtained by direct counts of change events. The proposed recovery method is an option when unit-level change is seriously compromised by errors. The choice of a 3×3 cluster was a compromise between conflicting goals. A larger cluster would be more robust against errors but would incur additional loss of information and increases in computational complexity. A smaller cluster, however, would be less robust against registration and classification errors without offering any significant computational advantages.

The Monte Carlo simulations confirmed the sensitivity of unit-level change estimates derived directly from remotely sensed data to errors of coregistration and classification (Bruzzone and Cossu 2003, Lunetta and Elvidge 1999). Average coregistration errors in the range of 0.3 to 1.1 units (pixels) are not uncommon. Classification accuracies of 0.7–0.9 units are commonly reported for forest cover-type maps derived from Landsat Enhanced Thematic Mapper+ (Foody 2002, Holmgren and

Thureson 1998). Thus, if no better approach to mitigate the bias is available, the proposed recovery should be pursued when classification accuracy and registration errors have the potential to seriously compromise the results.

Acknowledgments

Data for the IT site were kindly provided by Dr. P.M. Corona of the Università degli Studi della Tuscia in Italy.

Literature Cited

- Bruzzone, L.; Cossu, R. 2003. An adaptive approach to reducing noise effects in unsupervised change detection. *Geoscience and Remote Sensing*. 41(11): 2455-2465.
- Congalton, R.G. 2001. Accuracy assessment and validation of remotely sensed and other spatial information. *International Journal of Wildland Fire*. 10: 321-328.
- Coppin, P.R.; Bauer, M.E. 1996. Digital change detection in forest ecosystems with remote sensing imagery. *Remote Sensing of Environment*. 13: 207-234.
- Coppin, P.R.; Jonckheere, I.; Nackaerts, K.; Muys, B.; Lambin, E.F. 2004. Digital change detection methods in ecosystem monitoring: a review. *International Journal of Remote Sensing*. 25(9): 1565-1596.
- Czaplewski, R.L. 2003. Accuracy assessment of maps of forest conditions: statistical designs and methodological considerations. In: *Wulder, M.A.; Franklin, S.E., eds. Remote sensing of forest environments: concepts and case studies*. Boston: Kluwer Academic Publishers: 115-140.
- Fleiss, J.L. 1981. *Statistical methods for rates and proportions*. New York: John Wiley. 313 p.
- Foody, G.M. 2002. Status of land cover classification accuracy assessment. *Remote Sensing of Environment*. 80: 185-201.

-
- Holmgren, P.; Thureson, T. 1998. Satellite remote sensing for forestry planning—a review. *Scandinavian Journal of Forest Research*. 13: 90-110.
- Lunetta, R.S.; Elvidge, C.D. 1999. Remote sensing change detection: environmental monitoring methods and applications. London: Taylor & Francis. 318 p.
- Magnussen, S. 2004. Prediction of 2 x 2 tables of change from repeat cluster sampling of marginal counts. *Canadian Journal of Forest Research*. 34(8): 1703-1713.
- Magnussen, S. 2007. A method for estimation of a land cover change matrices from error-prone unit-level observations. *Canadian Journal of Forest Research*. 37(12): 1505-1517.
- Murtaugh, P.A.; Phillips, D.L. 1998. Temporal correlation of classification in remote sensing. *Journal of Agricultural, Biological and Environmental Statistics*. 3(1): 99-110.
- Pontius, R.G., Jr.; Lippitt, C.D. 2006. Can error explain map differences over time? *Cartography and Geographic Information Science*. 33(2): 159-171.
- Stehman, S.V.; Czaplewski, R.L. 1998. Design and analysis for thematic map accuracy assessment: fundamental principles. *Remote Sensing of Environment*. 64: 331-344.